

## Excitonic effects in linear and nonlinear optical properties of $C_{60}$

F. Bechstedt

*Department of Physics, University of California, San Diego, La Jolla, California 92093-0319  
and Institut für Festkörpertheorie und Theoretische Optik, Friedrich-Schiller-Universität, 07743 Jena, Germany*

M. Fiedler

*Institut für Festkörpertheorie und Theoretische Optik, Friedrich-Schiller-Universität, 07743 Jena, Germany*

L. J. Sham

*Department of Physics, University of California, San Diego, La Jolla, California 92093-0319*

(Received 7 July 1998; revised manuscript received 18 September 1998)

A model study of the singlet excitons in  $C_{60}$  with emphasis on the Coulomb interaction between an excited electron and hole and with the aid of the molecular symmetry leads to a physical understanding of the interaction effects on the absorption spectra and to an identification of the forbidden excitons in the third-harmonic generation spectra. These conclusions may be tested experimentally on the model predictions related to the optical Kerr effect. Briefly discussed is the application of the model to other molecules, small clusters, and quantum dots, with the possibility of an excitonic ground state. [S0163-1829(99)06904-0]

### I. INTRODUCTION

Since the discovery of  $C_{60}$ ,<sup>1</sup> several experimental and theoretical studies have suggested that undoped and doped  $C_{60}$  solids are strongly correlated electron systems. The observational basis includes the unusually high superconducting transition temperature of the alkali-metal-doped fullerites,<sup>2</sup> the existence of soft ferromagnetism,<sup>3</sup> the strong Coulomb interaction effects in the Auger spectrum, and direct and inverse photoemission.<sup>4</sup> The theoretical motivation is based on the narrow bandwidth compared to the strong intramolecular interaction. This naturally leads to theories based on the Hubbard model with an on-site interaction on every carbon atom.<sup>4-6</sup> The strong correlation is used to find a mechanism for superconductivity.<sup>7</sup> Parity doublets of the lowest unoccupied molecular orbitals (LUMO's) of the  $C_{60}$  molecule are used for the pairing mechanism.<sup>8</sup> The Coulomb interaction of the electrons within a single  $C_{60}$  molecule has also been taken into account through the configuration interaction by several quantum-chemistry calculations.<sup>9-12</sup> On the other hand, the quasiparticle correction<sup>13,14</sup> to the local-density approximation<sup>15,16</sup> leads to the conclusion that, while the correlation effect is large, the electronic structure in  $C_{60}$  is nonetheless that of a standard band insulator.<sup>14</sup> Similarly, the superconducting transition temperature of the alkali-doped  $C_{60}$  has been explained by the usual phonon mechanism.<sup>17,18</sup>

A common feature among the theories mentioned above is the assumption of the closed-shell ground state for  $C_{60}$  with the set of highest occupied molecular orbitals (HOMO's) of symmetry  $h_u$  and  $h_g$  and the set of LUMO's of symmetry  $t_{1u}$  and  $t_{1g}$ . We examine the Coulomb interaction effects on the excitation of an electron from a HOMO to a LUMO and the influence of the resultant excitons on the linear and nonlinear optical properties. The method of this study may be applied to other molecular solids, clusters, and quantum dots. In par-

ticular, our study of  $C_{60}$  may be used as a paradigm to investigate the stability of the closed-shell ground state against the excitons. By using a simple model, we hope to understand the factors governing such instability and to explore consequences, such as in nonlinear optical properties. Even if the excited states are only low in energy without causing any instability, they could play an interesting role in some properties, especially superconductivity.

First, we study the energy ordering of the closed-shell state and the one-electron-hole pair excited states. Shirley *et al.*<sup>19</sup> used a molecular orbital model to make a comprehensive study of the exciton energy spectrum in solid  $C_{60}$ . We adopt a similar approach, but use further simplifications. The excitons are not confined only to the optically active ones. We restrict our attention to excitations within a single  $C_{60}$  molecule since in the solid the weak overlapping between the molecules<sup>20</sup> would not qualitatively affect our results. However, the intermolecular screening effect is modeled by a dielectric constant. We use a nearest-neighbor tight-binding model for the one-electron  $\pi$  orbitals<sup>8,21,22</sup> with the help of symmetry considerations.<sup>23</sup> The essential results of the one-electron states are given in Sec. II. In Sec. III the energies of the electron-hole pair states relative to the closed-shell state are determined in terms of the single-particle energies and the Coulomb interaction. The interaction terms include direct electron-hole attraction and the exchange counterpart,<sup>24</sup> interaction on the same carbon site as well as between any pairs of carbon sites in the same  $C_{60}$  molecule. We examine the dependence of the pair-state energies on three model parameters, the nearest-neighbor hopping energy  $V$ , the intra-site interaction  $U$  (including both the direct and exchange contributions), and the typical long-range interaction term  $e^2/\epsilon R_0$ , taking into account the intersite screening effect  $\epsilon$  and setting the distance scale at the radius of the buckyball  $R_0$  ( $\approx 3.5$  Å).

Second, we study the effects of the excitons on the optical

properties. In Sec. IV our calculations of the linear optical spectra are compared with experiment and our calculations of the nonlinear properties are used to interpret the experiments on third harmonic generation and to suggest measurements that will test our theory. In Sec. V we summarize the results of our work on  $C_{60}$  and speculate on the possibility of small systems with an excitonic state as the ground state.

## II. SINGLE-PARTICLE EXCITATIONS

The first order of business is to construct the most relevant one-electron orbitals in  $C_{60}$ , namely, the HOMO's and LUMO's. Their approximation by  $\pi$  orbitals seems to be well established for low-energy excitations. For instance, the weights of the radial orbital for the  $h_u$  and  $t_{1u}$  states were about 98% and 95%, respectively, according to Laouini *et al.*<sup>25</sup> In the discussion of the electron-hole interaction the small  $\sigma$  contributions may be neglected. The tight-binding Hamiltonian with the nearest-neighbor hopping may be built from the molecular  $\pi$  orbitals:<sup>23</sup>

$$\phi_{lmp}(\mathbf{x}) = N_l \sum_{\mathbf{g}} e_{lmp}(\mathbf{g}) \chi(\mathbf{x} - R_0 \mathbf{g}), \quad (2.1)$$

where  $\chi(\mathbf{x} - R_0 \mathbf{g})$  is the component of the  $p$  wave function centered around the atomic sites  $R_0 \mathbf{g}$  pointing along the radial direction. We have neglected the difference in bond lengths of the inequivalent bonds.  $N_l$  gives the normalization of the molecule state. The quantum number  $l$  is used to index the irreducible representations<sup>26</sup> of the icosahedral group  $I_h$ , the symmetry group of the buckyball, namely  $a$ ,  $t_1$ ,  $h$ ,  $t_2$ , and  $g$ , with degeneracies 1, 3, 5, 3, and 4, respectively. The quantum number  $m$  runs over the degenerate states of each irreducible representation. The quantum number  $p$  denotes the parity of the state. Its introduction indicates that the full symmetry group of  $C_{60}$  is  $I_h \times Z_2$ , where  $Z_2$  is the two-element group consisting of the inversion operator and the identity. The coefficients for different sites may be related to each other by<sup>8</sup>

$$e_{lpm}(\mathbf{g}) = \sum_{m'=-l}^{+l} D_{mm'}^{l*}(\omega_{\mathbf{g}}) e_{lpm'}(\mathbf{e}), \quad (2.2)$$

where  $\omega_{\mathbf{g}}$  is the rotation bringing the radial vector from atomic site  $\mathbf{e}$  [see Fig. 1, not to be confused with the coefficients  $e_{lmp}(\mathbf{g})$ ] to site  $\mathbf{g}$ . For the regular three- and five-dimensional representations ( $l=1,2$ ) under consideration the  $(2l+1) \times (2l+1)$  matrices  $\hat{D}^l$  are simply the standard transformation matrices in a rigid body, the so-called Wigner  $D$  functions.<sup>27</sup>

The irreducible representations  $D_{mm'}^l(\omega_{\mathbf{g}})$  of the coefficients  $e_{lmp}(\mathbf{g})$  reduce the nearest-neighbor Hamiltonian in units of the hopping parameter  $-V$  to a set of Hamiltonians given by<sup>8</sup>

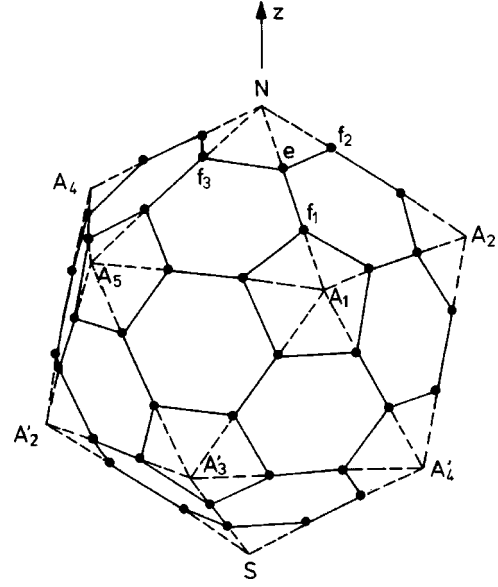


FIG. 1. Structure of the  $C_{60}$  molecule. Each dot denotes the position of a carbon atom. The connecting solid lines indicate the bonds. The intact icosahedron with the vertices at  $N$ ,  $S$ ,  $A_i$ , and  $A'_i$  ( $i=1, \dots, 5$ ) is indicated by the dashed lines.

$$h_{mm'}^l = \sum_{i=1}^3 D_{mm'}^{l*}(\omega_{f_i}), \quad (2.3)$$

where the sum only runs over the three nearest neighbors  $\mathbf{f}_i$  of the site  $\mathbf{e}$ . The spin degrees of freedom are understood. For readers interested in generating the irreducible representations,<sup>27</sup> we record the coordinates  $\mathbf{e} = \frac{1}{3}(R/R_0)[\sin(2\Theta_0), 0, 2 + \cos(2\Theta_0)]$ , where the angle  $2\Theta_0 = \cos^{-1}(1/\sqrt{5})$  is defined by the geodesic arc between two neighboring vertices of the icosahedron. The rotations to the nearest neighbors  $\mathbf{f}_i$  from the atom at  $\mathbf{e}$  are given by the Euler angles  $(\alpha=0, \beta=2\Theta_0, \gamma=\pi)$ ,  $(\alpha=2\pi/5, \beta=0, \gamma=0)$ , and  $(\alpha=-2\pi/5, \beta=0, \gamma=0)$ , respectively, for  $i=1, 2$ , and 3.

The LUMO's and HOMO's of interest belong to the representations  $t_1$  and  $h$ , respectively, which are isomorphous to the spherical harmonics  $l=1$  ( $p$  wave) and  $l=2$  ( $d$  wave). The state degeneracy is then  $2l+1$  and the normalization  $N_l = \sqrt{(2l+1)/60}$ . The corresponding Hamiltonians for these states are

$$\hat{h}^1 = \begin{pmatrix} -1 + \frac{2}{\sqrt{5}} & -\sqrt{\frac{2}{5}} & -\frac{1}{2} \left(1 - \frac{1}{\sqrt{5}}\right) \\ -\sqrt{\frac{2}{5}} & 2 + \frac{1}{\sqrt{5}} & \sqrt{\frac{2}{5}} \\ -\frac{1}{2} \left(1 - \frac{1}{\sqrt{5}}\right) & \sqrt{\frac{2}{5}} & -1 + \frac{2}{\sqrt{5}} \end{pmatrix},$$

$$\hat{h}^2 = \begin{pmatrix} -\frac{1}{5} - \frac{2}{\sqrt{5}} & \frac{1}{\sqrt{5}} + \frac{1}{5} & \frac{\sqrt{6}}{5} & \frac{1}{\sqrt{5}} - \frac{1}{5} & \frac{3}{10} - \frac{1}{2\sqrt{5}} \\ \frac{1}{\sqrt{5}} + \frac{1}{5} & -\frac{1}{5} + \frac{2}{\sqrt{5}} & -\frac{\sqrt{6}}{5} & -\frac{3}{10} - \frac{1}{2\sqrt{5}} & -\frac{1}{\sqrt{5}} + \frac{1}{5} \\ \frac{\sqrt{6}}{5} & -\frac{\sqrt{6}}{5} & \frac{9}{5} & \frac{\sqrt{6}}{5} & \frac{\sqrt{6}}{5} \\ \frac{1}{\sqrt{5}} - \frac{1}{5} & -\frac{3}{10} - \frac{1}{2\sqrt{5}} & \frac{\sqrt{6}}{5} & -\frac{1}{5} + \frac{2}{\sqrt{5}} & -\frac{1}{\sqrt{5}} - \frac{1}{5} \\ \frac{3}{10} - \frac{1}{2\sqrt{5}} & -\frac{1}{\sqrt{5}} + \frac{1}{5} & \frac{\sqrt{6}}{5} & -\frac{1}{\sqrt{5}} - \frac{1}{5} & -\frac{1}{5} - \frac{2}{\sqrt{5}} \end{pmatrix}, \quad (2.4)$$

where  $\cos(2\Theta_0)=1/\sqrt{5}$  and  $\cos(2\pi/5)=(-1+\sqrt{5})/4$  are used.

The eigenvalues  $\lambda$  of the reduced Hamiltonians for the two LUMO and two HOMO levels are in closed form

$$\lambda_{1+} = \frac{1}{2}(-3 + \sqrt{5}),$$

$$\lambda_{1-} = \frac{1}{2}[(3 + \sqrt{5})/2 - \sqrt{(19 - \sqrt{5})/2}] \quad (2.5)$$

for  $l=1$  and

$$\lambda_{2-} = \frac{1}{2}(-1 + \sqrt{5}),$$

$$\lambda_{2+} = 1 \quad (2.6)$$

for  $l=2$ , in agreement with other calculations.<sup>8,22,23</sup> These orbitals are associated, respectively, with the symmetry  $t_{1g}$ ,  $t_{1u}$ ,  $h_u$ , and  $h_g$ . The single-particle energies of these molecule states are

$$\varepsilon_{lp} = -\lambda_{lp}V, \quad (2.7)$$

where  $lp$  runs over the indices  $1+$  (for the representation  $t_{1g}$ ),  $1-$  ( $t_{1u}$ ),  $2-$  ( $h_u$ ), and  $2+$  ( $h_g$ ). The normalized eigenvectors with  $(2l+1)$  components at carbon site  $\mathbf{e}$  are given by (with  $x=\lambda_{1-}-2-1/\sqrt{5}$  and  $\tan y=\sqrt{5}x/2$ )

$$\hat{e}_{1+}(\mathbf{e}) = \frac{1}{\sqrt{2}} \begin{pmatrix} 1 \\ 0 \\ 1 \end{pmatrix}, \quad \hat{e}_{1-}(\mathbf{e}) = \frac{1}{\sqrt{2}} \begin{pmatrix} -\sin y \\ \sqrt{2} \cos y \\ \sin y \end{pmatrix},$$

$$\hat{e}_{2-}(\mathbf{e}) = \frac{1}{\sqrt{10}} \begin{pmatrix} 1 \\ 2 \\ 0 \\ 2 \\ -1 \end{pmatrix}, \quad \hat{e}_{2+}(\mathbf{e}) = \frac{1}{\sqrt{30}} \begin{pmatrix} -1 + \sqrt{5} \\ 1 + \sqrt{5} \\ \sqrt{6} \\ -1 - \sqrt{5} \\ -1 + \sqrt{5} \end{pmatrix}, \quad (2.8)$$

triplets for the LUMO states and quintets for the HOMO states. The complete eigenvectors with the components for the other atoms follow by rotation (2.2). Using this equation, the definition of the Wigner  $D$  functions,<sup>27</sup> and the form of the vectors in Eq. (2.8) one can easily show the parity of the states  $e_{lm\pm}(-\mathbf{g}) = \pm e_{lm\pm}(\mathbf{g})$ . The pairs of vectors for the atoms at the sites  $\mathbf{e}$  and  $-\mathbf{e}$  give instructive examples. The corresponding transformation matrices  $D_{mm'}^l(0, \pi, 0) = (-1)^{l+m} \delta_{m, -m'}$  give eigenvectors at  $-\mathbf{e}$ , which fulfill the parity condition. Since the rigid-body transformation from  $\mathbf{e}$  to  $-\mathbf{g}$  may be related to a product of transformations from  $\mathbf{e}$  to  $\mathbf{g}$  and  $\mathbf{e}$  to  $-\mathbf{e}$ , the above property is also valid for arbitrary atomic positions  $\mathbf{g}$ .

Figure 2 shows schematically the two LUMO levels and two HOMO levels and their associated states. The energy scale is set by the hopping matrix element  $V$  in Eq. (2.7). The single-particle energy difference ( $\varepsilon_{1-} - \varepsilon_{2-}$ ) is taken to be 3.5 eV between  $t_{1u}$  and  $h_u$  peaks in solid  $C_{60}$  measured by the photoemission and inverse-photoemission experiments.<sup>4,28,29</sup> This yields an estimate of  $V=4.626$  eV. This value is bracketed by  $V=3.83$  and 6.61 eV representing the uncertainty of the estimate. The lower value follows from the energy difference taken at the midpoint between the band onset at 2.3 eV (Ref. 4) and the peak-to-peak difference at 3.5 eV to allow for the finite bandwidths in the solid. The higher value of  $V$  comes from the estimate of 5 eV as the difference between the electron affinity level and the ionization potential of the  $C_{60}$  molecule.<sup>30</sup> The three values of  $V$

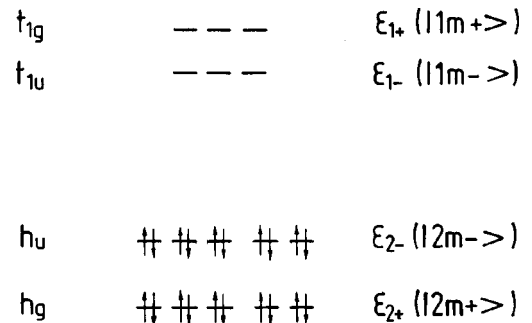


FIG. 2. Schematic four-level diagram of HOMO and LUMO states for characterization of the lowest electronic excitations in the  $C_{60}$  molecule.

yield the single-particle excitation spectrum  $\varepsilon_{1+}=4.63$  (3.83 and 6.61) eV ( $t_{1g}$ ),  $\varepsilon_{1-}=3.50$  (2.90 and 5.00) eV ( $t_{1u}$ ),  $\varepsilon_{2-}=0$  eV ( $h_u$ ), and  $\varepsilon_{2+}=-1.77$  (-1.46 and -2.52) eV ( $h_g$ ), with respect to the position of the highest occupied state. The discrepancy between these values of  $V$  and the local-density approximation derived  $V=2.72$  eV (Ref. 25) represents the phenomenological fit of the former to the renormalized one-particle energies so that, when the interaction between two single-particle excitations is considered later, the one-particle energies should not be further modified by the interaction.

### III. EXCITONS

#### A. Symmetry-adapted electron-hole pair states

In this paper we shall consider only electron-hole excitations without spin flip, i.e., only singlet excitons. We have calculated the energies of the triplet excitons, which, devoid of exchange interaction, lie slightly lower than the singlets.<sup>19</sup> The possibility of magnetism involving the triplet state will be left to a future study.

Consideration of the electron-hole pair excitations of the  $\pi$ -electron system of  $C_{60}$ , which are lowest in energy, can be restricted to the level scheme of Fig. 2 with the empty levels  $t_{1g}$  and  $t_{1u}$  and the occupied states  $h_u$  and  $h_g$ . The pair excitations contain products of the type  $t_{1p_e} \times h_{p_h}$  with the single-particle parities  $p_e, p_h = +1(g)$  or  $-1(u)$ . With the pair parity  $P = p_e p_h$ , where  $P$  runs over the same values  $+1(G)$  and  $-1(U)$  as  $p_e$  and  $p_h$ , the pair states have the symmetry<sup>10</sup>

$$t_{1p_e} \times h_{p_h} = T_{1P} + T_{2P} + G_P + H_P. \quad (3.1)$$

That is, each of these four 15-dimensional product representations of a singlet electron-hole pair from LUMO/HOMO of the type  $h_{p_h} \rightarrow t_{1p_e}$  splits up into two three-dimensional representations  $T_{1P}$  and  $T_{2P}$ , one four-dimensional  $G_P$  representation, and one five-dimensional  $H_P$  representation ( $P = G, U$ ).<sup>31</sup> Among them are the dipole-allowed pair excitations  $T_{1U}$  for an electron and a hole with opposite parity. For these optically observable excitons, there is no need to consider the fourfold degenerated  $g_g$  hole level, which is either somewhat below the  $h_g$  level<sup>10</sup> or degenerate with it within the approximations considered,<sup>8,22,23</sup> from the relation<sup>10</sup>

$$t_{1p_e} \times g_g = T_{2P} + G_P + H_P, \quad (3.2)$$

which contains no representation  $T_{1U}$  of the electric-dipole-allowed excitons. Symmetry reasons also dictate that there is no configurational interaction between the  $A_G$  ground state and the low-lying pair states considered.

We develop a method of computing the excitonic states in terms of the symmetry-adapted electron-hole pair states (and incidentally gained some physical insight into these pair states) by exploiting the close relation of the representations of the symmetry group  $I_h$  of the  $C_{60}$  molecule with the transformation properties of the spherical harmonics<sup>23</sup> that differ by a small perturbation. The  $t_{1p_e}$  of the LUMO and the  $h_{p_h}$  of the HOMO correspond to single-particle angular momentum states with the quantum numbers  $l$  and  $m$  ( $l=1,2$  and  $-l \leq m \leq l$ ). The angular momentum addition rules would

yield the symmetry of the resulting electron-hole pair states to be those of the spherical harmonics  $L$  and  $M$  with  $L=1,2,3$  and  $-L \leq M \leq L$ . Indeed, the pair states have a three-dimensional representation  $T_{1P}$  corresponding to  $L=1$  and a five-dimensional representation  $H_P$  corresponding to  $L=2$ . However, since  $C_{60}$  does not have complete spherical symmetry, the  $L=3$  states split into two groups, a three-dimensional representation  $T_{2P}$  and a four-dimensional one  $G_P$ . The symmetry-adapted electron-hole pair spin-singlet states may be written as linear combinations

$$|LNp_e p_h\rangle = \sum_{m_e=-1}^1 \sum_{m_h=-2}^2 C_{m_e m_h}^{12}(LN) c_{1p_e m_e}^\dagger c_{2p_h m_h} |0\rangle, \quad (3.3)$$

where the operator  $c_{lpm}^\dagger (c_{lpm})$  creates (annihilates) an electron in a molecule state  $|lpm\rangle$  with a single-particle parity  $p$ . The coefficients on the right-hand side of Eq. (3.3) are related to the Clebsch-Gordan coefficients  $C_{lm'l'm'}^{LM}$  (Ref. 27) by ( $L=1,2$  with  $-L \leq N \leq L$  and  $L=3$  with  $N=0, \pm 1$ )

$$C_{m_e m_h}^{12}(LN) = (-1)^{-m_h} C_{1m_e 2-m_h}^{LN},$$

$$C_{m_e m_h}^{12}(3, \pm 3) = (-1)^{-m_h} \left[ \sqrt{\frac{2}{5}} C_{1m_e 2-m_h}^{3 \pm 3} \pm \sqrt{\frac{3}{5}} C_{1m_e 2-m_h}^{3 \mp 2} \right],$$

$$C_{m_e m_h}^{12}(3, \pm 2) = (-1)^{-m_h} \left[ \sqrt{\frac{2}{5}} C_{1m_e 2-m_h}^{3 \mp 2} \mp \sqrt{\frac{3}{5}} C_{1m_e 2-m_h}^{3 \pm 3} \right]. \quad (3.4)$$

The symmetry-adapted pair states are chosen such that  $L=1$  corresponds to the basis of the irreducible representation  $T_{1P}$ ,  $L=2$  to  $H_P$ ,  $L=3$  and  $N=0, \pm 3$  to  $T_{2P}$ , and  $L=3$  and  $N=\pm 1, \pm 2$  to  $G_P$ .

The true singlet exciton states are linear combinations of the symmetry-adapted pair states (3.3)

$$|LNp\Lambda\rangle = \sum_{p=+,-} c_{\Lambda p}(LNP) |LN(Pp)p\rangle, \quad (3.5)$$

where the summation runs over the hole parity  $p$ . The summation in Eq. (3.5) indicates that pair states of different single-particle parities may be coupled provided the total parity  $P$  is conserved. The fourth quantum number  $\Lambda$  labels the two coupled pair states of the same symmetry. The four quantum numbers  $L, N, P$ , and  $\Lambda$  span the 60 pair states (without spin) under consideration. The eigenstates (3.5) of the Frenkel excitons are orthonormalized with  $\sum_p c_{\Lambda p}^* c_{\Lambda' p} = \delta_{\Lambda \Lambda'}$ , following the orthonormal property of the Clebsch-Gordan coefficients.

The symmetry-adapted basis pair states  $|LN(Pp)p\rangle$  of Eq. (3.3) with the third quantum number set to  $p_e = Pp$  block diagonalize the two-body Hamiltonian of the  $\pi$ -electron system including the full Coulomb interaction  $v$  into  $2 \times 2$  matrices diagonal in the quantum numbers  $L, N$ , and  $P$ :

$$\begin{aligned} \langle LN(Pp)p | H | L'N'(P'p')p' \rangle \\ = \delta_{LL'} \delta_{NN'} \delta_{PP'} \{ \delta_{pp'} [\varepsilon_{1Pp} - \varepsilon_{2Pp}] \\ + \langle LN(Pp)p | v | LN(P'p')p' \rangle \}, \end{aligned} \quad (3.6)$$

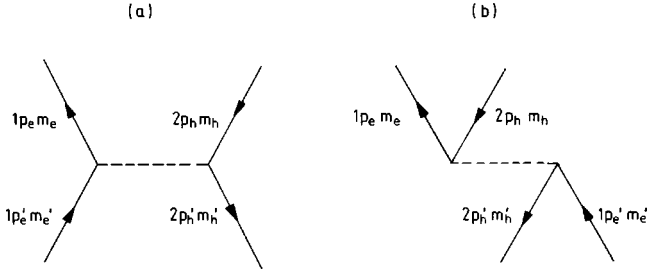


FIG. 3. Feynman diagrams for the electron (upward arrows)-hole (downward arrows) interaction (dashed line): (a) the direct attraction and (b) the exchange counterpart.

with the electron in the level with the excitation energy  $\varepsilon_{1p_e}$ , the hole in the level with  $\varepsilon_{2p_h}$ , and the Coulomb interaction connecting pair states with  $(p_e, p_h)$  and  $(-p_e, -p_h)$ . In our notation system, the exciton energy eigenvalues  $E_{LNPA}$  are independent of  $N$  for  $L=1,2$ , i.e.,  $(2L+1)$ -fold degenerate. For  $L=3$ , the exciton energies for the two symmetry sets of  $N=0, \pm 3$  and  $N=\pm 1, \pm 2$  are different but degenerate within each set.

### B. Coulomb interaction

The Coulomb interaction term in Eq. (3.6) includes the electron-hole attraction and the exchange term to the electron-hole attraction<sup>24</sup> with the diagrammatic representation in Fig. 3. The exchange terms of Fig. 3(b) only exist for the spin-singlet exciton. Assuming nonoverlap of the  $p_z$  orbitals from different carbon sites of the  $\pi$ -like molecule states, we express the Coulomb term in Eq. (3.6) in terms of the single-particle eigenstates of Eqs. (2.2) and (2.8) as

$$\begin{aligned} & \langle LNp_e p_h | v | LNp'_e p'_h \rangle \\ &= -\frac{15}{(60)^2} \sum_{g, g'} G_{LN}^*(12p_e p_h | \mathbf{g}\mathbf{g}') v(\mathbf{g}-\mathbf{g}') \\ & \quad \times G_{LN}(12p'_e p'_h | \mathbf{g}\mathbf{g}') \\ & + 2\frac{15}{(60)^2} \sum_{g, g'} G_{LN}^*(12p_e p_h | \mathbf{g}\mathbf{g}') v(\mathbf{g}-\mathbf{g}') \\ & \quad \times G_{LN}(12p'_e p'_h | \mathbf{g}'\mathbf{g}'), \end{aligned} \quad (3.7)$$

with

$$\begin{aligned} & G_{LN}(l_e l_h p_e p_h | \mathbf{g}\mathbf{g}') \\ &= \sum_{m_e=-l_e}^{+l_e} \sum_{m_h=-l_h}^{+l_h} C_{m_e m_h}^{l_e l_h}(LN) e_{l_e p_e m_e}^*(\mathbf{g}) e_{l_h p_h m_h}(\mathbf{g}'), \end{aligned} \quad (3.8)$$

where the coefficients  $C_{m_e m_h}^{l_e l_h}(LN)$  are defined in Eq. (3.4). The Coulomb potential takes the form

$$v(\mathbf{g}) = U \delta_{g0} + \frac{e^2}{\epsilon R_0} \frac{1}{|\mathbf{g}|} (1 - \delta_{g0}), \quad (3.9)$$

where  $U$  denotes the on-site Coulomb matrix element of the  $p_z$  orbitals, which should be reduced by the correlation with

the  $\sigma$  electrons.<sup>32</sup>  $R_0$  is the distance from a carbon atom to the center of the cage and  $\epsilon$  denotes a dielectric constant representing the screening of the interatomic (but intramolecule) Coulomb interaction. Strictly speaking, the screening of the Coulomb potential in the direct term includes a contribution from the excitons under consideration that is absent in the exchange term.<sup>24</sup> Our approximation is valid if the contributions from the dynamics of the  $\sigma$  electrons<sup>32</sup> and other  $C_{60}$  molecules dominate.

The first term on the right-hand side of Eq. (3.7) comes from the direct electron-hole attraction and the second is the exchange counterpart. The factor of 2 may be viewed as originating from the spin degeneracy or the structure of the singlet. The double sums over the carbon sites in the expression (3.7) may be reduced to single sums by means of the product relation for the Wigner  $D$  functions representing the two rigid-body transformations to the sites. Thus, with a simplifying definition for the Coulomb matrix element

$$\begin{aligned} V_{pp'}(LNP) &\equiv -\langle LN(Pp)p | v | LN(Pp')p' \rangle \\ &= -\frac{U}{60} F_{pp'}(LNP) \\ & \quad + \frac{e^2}{\epsilon R_0} [H_{pp'}(LNP) - 2X_{pp'}(LNP)], \end{aligned} \quad (3.10)$$

where the  $N$  dependence serves only to differentiate between  $T_{2P}$  and  $G_P$  in the  $L=3$  case. For  $L=1,2$  ( $-L \leq N \leq L$ ) and  $L=3$  ( $N=0, \pm 1$ ), the intra-atomic Coulomb interaction is given by

$$\begin{aligned} F_{pp'}(LNP) &= \frac{15}{2L+1} \sum_{M=-L}^{+L} \\ & \quad \times G_{LM}^*(12(Pp)p | \mathbf{e}\mathbf{e}) G_{LM}(12(Pp')p' | \mathbf{e}\mathbf{e}) \end{aligned} \quad (3.11)$$

and the interatomic Hartree and exchange contributions

$$\begin{aligned} H_{pp'}(LNP) &= \frac{1}{4(2L+1)} \sum_{M=-L}^{+L} \sum_g' G_{LM}^*(12(Pp)p | \mathbf{g}\mathbf{e}) \\ & \quad \times \frac{1}{|\mathbf{g}-\mathbf{e}|} G_{LM}(12(Pp')p' | \mathbf{g}\mathbf{e}), \end{aligned} \quad (3.12)$$

$$\begin{aligned} X_{pp'}(LNP) &= \frac{1}{4(2L+1)} \sum_{M=-L}^{+L} \sum_g' G_{LM}^*(12(Pp)p | \mathbf{g}\mathbf{g}) \\ & \quad \times \frac{1}{|\mathbf{g}-\mathbf{e}|} G_{LM}(12(Pp')p' | \mathbf{e}\mathbf{e}), \end{aligned} \quad (3.13)$$

where the functions  $G_{LM}$  are defined in Eq. (3.8). The intra-atomic term (3.11) includes both the Hartree and exchange contributions.

In Table I are listed the values of these three terms evaluated from Eqs. (3.11)–(3.13). The corresponding results using the continuum approximation of Ref. 8 differ little for the Hartree contributions, but up to 50% for the exchange terms. Table I indicates that the interatomic electron-hole exchange

TABLE I. Intra-atomic and interatomic Coulomb interaction matrix elements (3.11, 3.12, 3.13). (I.R. denotes irreducible representation.)

| IR       | Quantum numbers |                   |     | $F_{pp'}(LNP)$ |         |          | $H_{pp'}(LNP)$ |         |          | $X_{pp'}(LNP)$ |          |          |
|----------|-----------------|-------------------|-----|----------------|---------|----------|----------------|---------|----------|----------------|----------|----------|
|          | $L$             | $N$               | $P$ | ++             | --      | +-       | ++             | --      | +-       | ++             | --       | +-       |
| $T_{1G}$ | 1               | $0, \pm 1$        | 1   | 0.50000        | 0.76690 | 0.61923  | 0.87251        | 0.89689 | 0.22713  | -0.02111       | -0.03239 | -0.02615 |
| $H_G$    | 2               | $0, \pm 1, \pm 2$ | 1   | 1.50000        | 1.23310 | 0.79877  | 0.85182        | 0.82745 | 0.05389  | 0.03329        | 0.04047  | 0.05790  |
| $T_{2G}$ | 3               | $0, \pm 3$        | 1   | 1.33333        | 1.99975 | -1.63289 | 0.85527        | 0.87308 | -0.09762 | -0.08122       | -0.12181 | 0.09947  |
| $G_G$    | 3               | $\pm 1, \pm 2$    | 1   | 0.50000        | 0.13364 | -0.23822 | 0.87251        | 0.87134 | -0.16449 | -0.00908       | -0.00303 | 0.00416  |
| $T_{1U}$ | 1               | $0, \pm 1$        | -1  | 1.54204        | 1.50000 | 1.50777  | 0.85363        | 0.84560 | 0.19439  | 0.16148        | 0.11124  | 0.13512  |
| $H_U$    | 2               | $0, \pm 1, \pm 2$ | -1  | 0.45796        | 0.50000 | -0.08977 | 0.87070        | 0.87873 | 0.08662  | -0.01309       | -0.02673 | 0.00445  |
| $T_{2U}$ | 3               | $0, \pm 3$        | -1  | 0.63864        | 1.00000 | 0.21489  | 0.86786        | 0.91547 | -0.18339 | 0.02377        | -0.01409 | 0.01251  |
| $G_U$    | 3               | $\pm 1, \pm 2$    | -1  | 1.54204        | 1.25000 | -1.17978 | 0.85363        | 0.81391 | -0.11652 | -0.06371       | -0.07559 | 0.07082  |

may be neglected in comparison to the interatomic electron-hole attraction. This is in complete contrast to the intra-atomic case, which is exchange dominated since the singlet exciton has twice the number of exchange terms of equal magnitude as the direct attraction (cf. Fig. 3). Since the prefactor  $U/60$  is smaller than  $e^2/\epsilon R_0$ , it is evident that the diagonal elements  $V_{pp}(LNP)$  in Eq. (3.10) are dominated by the interatomic Hartree matrix elements and are therefore positive. The off-diagonal elements  $p \neq p'$  are strongly influenced by the intra-atomic exchange. They are often negative (except for  $T_{1G}$  and  $H_U$ ). Table I also shows that a contact-potential approximation, where the interatomic Coulomb interactions are neglected, is invalid.

### C. Pair excitation energies and ground-state stability

With the Coulomb interaction given in Table I, the  $2 \times 2$  eigenvalue problems for the 60 Frenkel excitons originated from the closest  $\pi$ -electron-related HOMO and LUMO single-particle states can be solved. For a given representation  $T_1, H, T_2$ , or  $G$  and a given total parity  $P = \pm 1$ , the  $2 \times 2$  Hamiltonian for hole states of parities  $p$  and  $p'$  may be written as

$$H_{pp'} = (\bar{E} + p\Delta) \delta_{pp'} - \tilde{U}(1 - \delta_{pp'}), \quad (3.14)$$

where

$$\begin{aligned} \bar{E} &= \frac{1}{2}(E_+ + E_-), \\ \Delta &= \frac{1}{2}(E_+ - E_-), \\ \tilde{U} &= V_{+-}(LNP), \end{aligned} \quad (3.15)$$

$$E_p = \varepsilon_{1(pP)} - \varepsilon_{2p} - V_{pp}(LNP).$$

The two exciton eigenvalues  $E_{LNP\Lambda}$  with  $\Lambda = \pm 1$  and the corresponding eigenvectors follow as

$$\begin{aligned} E_{LNP\Lambda} &= \bar{E} + \Lambda \sqrt{\Delta^2 + \tilde{U}^2}, \\ c_{\Lambda P}(LNP) &= \delta_{\Lambda P, +} \cos \eta + \delta_{\Lambda P, -} p \sin \eta, \end{aligned} \quad (3.16)$$

where

$$\sin(2\eta) = \tilde{U} / \sqrt{\Delta^2 + \tilde{U}^2}. \quad (3.17)$$

The coupling of the Frenkel excitons with the same representation and parity  $P$  destroys the simple picture that the reduction of the difference of the single-particle energies  $\varepsilon_{1Pp} - \varepsilon_{2p}$  in Eq. (3.15) by  $V_{pp}$  defines the binding energy of the exciton. The ratio  $\tilde{U} / \sqrt{\Delta^2 + \tilde{U}^2}$  determines the strength of the redistribution of the two coupled excitons with  $\Lambda = \pm 1$ . Therefore, the sign of  $\tilde{U}$  plays an important role for the actual oscillator strength for the excitations of electron-hole pairs with different  $\Lambda$ , as will be discussed in Sec. IV B.

In Figs. 4 and 5 a selected set of pair excitation energies is plotted versus the strength of the interatomic Coulomb interaction  $e^2/\epsilon R_0$  for two different values of the intrasite Coulomb matrix element  $U$ . To avoid clutter in Fig. 4, plotted are only excitons of representations  $T_{1P}(L=1)$  and  $H_P(L=2)$ , i.e., a total of eight exciton energies with  $P = \pm 1$  and  $\Lambda = \pm 1$ . The other eight exciton energies for the representations  $T_{2P}$  and  $G_P(L=3)$  are not plotted since they do not usually appear in the optical spectra considered below. Fig.

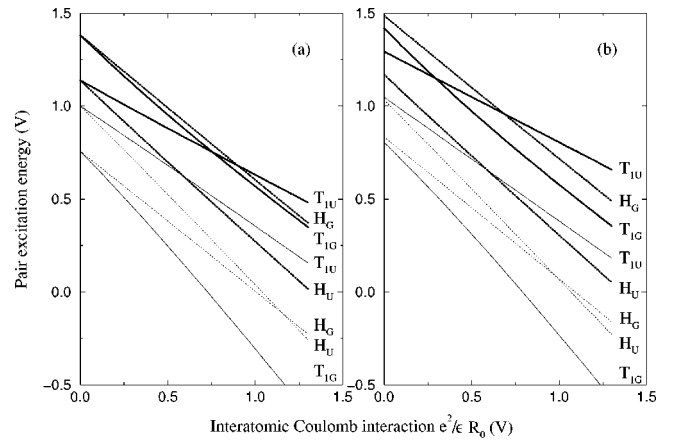


FIG. 4. Excitation energies of Frenkel excitons belonging to the single-particle pairs  $h_u \rightarrow t_{1u}$ ,  $h_u \rightarrow t_{1g}$ ,  $h_g \rightarrow t_{1u}$ , and  $h_g \rightarrow t_{1g}$  versus the effective interatomic Coulomb interaction strength  $e^2/\epsilon R_0$ . The intra-atomic Coulomb interaction is fixed at two values (a)  $U = 0$  and (b)  $U = 4V$ .  $T_{1P}$ , solid line;  $H_P$ , dashed line. Both parities  $P = +, -$  are considered. The high-energy (low-energy) solutions of the coupled pairs  $\Lambda = +$  ( $\Lambda = -$ ) are plotted as thick (thin) lines. All energies are given in units of the hopping parameter  $V$ .

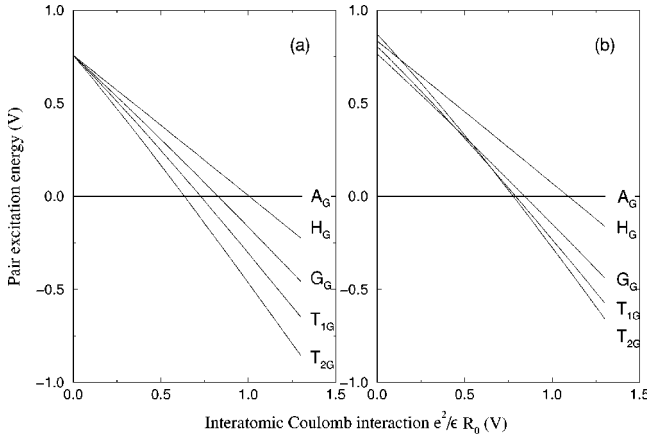


FIG. 5. Lowest even-parity exciton energies versus the interatomic Coulomb interaction. The zero line is given by the closed-shell Hartree-Fock ground state. (a)  $U=0$  and (b)  $U=4V$ .

Figure 5 compares the four lowest pair excitations  $T_{1G}$ ,  $T_{2G}$ ,  $G_G$ , and  $H_G$  with the  $A_G$  Hartree-Fock ground state with even parity. The two intra-atomic interaction values chosen are  $U=0$  and  $U=4V$ . The Coulomb energy  $U$  when two electrons are in the same atomic  $p$  orbital is usually estimated to be  $U \approx 10\text{--}20$  eV. If one uses a hydrogen-like wave function with an effective nuclear charge  $z_{eff} = 3.25$ , a value of  $U = 17.3$  eV results,<sup>8</sup> which is close to  $U=4V$  for the median value of  $V$  in Sec. II. If the effect of the  $\sigma$  electrons is included,  $U$  is reduced to 11 eV.<sup>32</sup> Both Figs. 4 and 5 show that the explicitly chosen  $U$  value has a minor influence on the excitation energies. A strong intra-atomic Coulomb interaction  $U=4V$  shifts the pair energies slightly to higher energies by about  $0.05V$ .

The dependence on the variation of the interatomic Coulomb interaction  $e^2/\epsilon R_0$  is explored because of the uncertainty of the value for the dielectric constant used to screen the interatomic interaction. The intramolecular correlation effects with the  $\sigma$  electrons<sup>32</sup> gives  $\epsilon = 1.5$ , which may be regarded as the minimum screening. With  $R_0 \approx 3.5$  Å and the smallest hopping parameter  $V$  in Sec. II, the maximum value of  $e^2/\epsilon R_0 V$  is about 0.7. In the literature, screening values between 3 and 10 have been reported. For instance, dielectric constants for solid fullerenes have been determined as  $\epsilon = 3.5, 3.9$ , or  $4.4$ .<sup>33–35</sup> A dielectric constant in a model cluster of 7.13–9.86 has been used in Ref. 36 to study the van der Waals cohesion energy. Other authors<sup>37</sup> use  $\epsilon = 4.4$  and 6.5 to explain the screening in  $C_{60}$  clusters. Hansen *et al.*<sup>38</sup> reported a value  $\epsilon = 4.6$  derived from a Kramers-Kronig analysis of their visible-UV electron-energy-loss spectrum. For  $\epsilon = 4.6$ , the interaction parameters of  $e^2/\epsilon R_0 V \approx 0.19$  (0.23 and 0.14) result from  $V = 4.626$  (3.83 and 6.61) eV. From Fig. 4, evidently the interatomic Coulomb interaction has much more influence on the pair-excitation energies than the on-site Coulomb interaction. Moreover, its presence gives rise to an effective attractive interaction between electrons and holes. The exciton binding noticeably reduces the pair excitation energies. Typical reductions amount to about  $0.8e^2/\epsilon R_0$  for  $T_{1G}$ ,  $H_G$ ,  $H_U$ , and  $G_G$  and vanishing intra-atomic interaction  $U$ . For  $T_{1U}$  ( $T_{2G}$ ), slightly smaller (larger) values of 0.5 (1.0)

$e^2/\epsilon R_0$  are shown in Figs. 4 and 5. The reductions corresponding to finite  $U$  values are smaller.

The findings in Figs. 4 and 5 can be compared with the results of quantum-chemical calculations for the  $C_{60}$  molecule<sup>10–12</sup> if the screening is taken to be entirely intramolecular. The quantum-chemical energies of the  ${}^1T_{1G}$ ,  ${}^1T_{2G}$ , and  ${}^1G_G$  multiplets are quasidegenerate, within a range of 0.1 eV, at about 0.5 eV, and the  ${}^1H_G$  multiplet is higher, separated by about 0.4 eV. Figure 5(b) ( $U=4V$ ) indicates a similar situation for the reasonable parameter value of  $e^2/\epsilon R_0 V \approx 0.7$  discussed above.

For solids, let us take  $\epsilon = 4.6$ . Then  $U = 17.3$  eV and  $V = 4.626$  (3.83 and 6.61) eV yield energy values 2.86 (2.53 and 3.90) eV for  $T_{1G}$ , 3.06 (2.65 and 4.24) eV for  $T_{2G}$ , 2.75 (2.46 and 3.71) eV for  $G_G$ , and 3.16 (2.71 and 4.41) eV for  $H_G$ . The resulting picture is more or less consistent with quasiparticle calculations for solid  $C_{60}$ ,<sup>14</sup> which yield the lowest excitation energy of 2.15 eV for the  $h_u \rightarrow t_{1u}$  transition. When the electron-hole interaction is included<sup>39</sup> this value is reduced to 1.57 eV, giving an exciton binding energy of 0.58 eV. This *ab initio* band calculation also gives peak positions for  $T_{2G}$ ,  $T_{1G}$ ,  $G_G$ , and  $H_G$  that are redshifted in comparison to the peak positions 1.86, 1.94, 2.03, and 2.30 eV in the fine structure of the forbidden absorption edge of the fullerite.<sup>39</sup> An inconsistency among the first-principles calculations is the energy ordering of the  $T_{1G}$  and  $T_{2G}$  excitations. In Refs. 10 and 11 the symmetry of the lowest excitation is  $T_{1G}$ , whereas other calculations<sup>12,39</sup> indicate the  $T_{2G}$  level to be the lowest one. Figure 5 shows that the answer depends on the relative strengths of the intra- and interatomic Coulomb interactions. For  $U=0$ ,  $T_{2G}$  represents the lowest excited state. For  $U=4V$ , this holds only for  $e^2/\epsilon R_0 V \geq 0.7$ . In the more interesting region of lower interatomic values  $T_{1G}$  is favored. For even smaller values of interatomic interaction,  $G_G$  becomes the lowest excited state.

## IV. OPTICAL SPECTRA

### A. Optical transitions

The coupling of light to the  $\pi$ -electron system of the  $C_{60}$  molecule is governed by the polarization operator

$$\hat{P}_\alpha = \sum_{\nu, \nu'} \langle \nu | e x_\alpha | \nu' \rangle c_\nu^\dagger c_{\nu'}, \quad (4.1)$$

where  $x_\alpha$  is the  $\alpha$ th Cartesian component of the position operator. With the restriction to the LUMO and HOMO states described in Sec. II and a strong localization of the  $p_z$  orbitals as in the case of the description of the Coulomb interaction in Eq. (3.9), the dipole matrix elements take the form ( $\nu \equiv lpm$ )

$$\begin{aligned} \langle lpm | e x_\alpha | l'p'm' \rangle \\ = eR_0 \frac{\sqrt{(2l+1)(2l'+1)}}{60} \sum_{\mathbf{g}} e_{lpm}^*(\mathbf{g}) g_\alpha e_{l'p'm'}(\mathbf{g}). \end{aligned} \quad (4.2)$$

The sum over the carbon positions can be evaluated using the symmetry properties<sup>27</sup>

$$\begin{aligned} \langle lpm|ex_\alpha|l'p'm'\rangle &= \delta_{p,-p'}D(l'l|pp') \\ &\times \sum_{M=-1}^{+1} (-1)^{m'} C_{lm'l'-m'}^{1M} A_{\alpha M}^1, \end{aligned} \quad (4.3)$$

where the effective dipole moment is given by

$$\begin{aligned} D(l'l|pp') &= eR_0 \frac{\sqrt{(2l+1)(2l'+1)}}{3} \\ &\times [-\sqrt{2}G_{11}(l'l|pp')|\mathbf{ee}]e_x \\ &+ G_{10}(l'l|pp')|\mathbf{ee}]e_z, \end{aligned} \quad (4.4)$$

with  $G_{LN}(l'l|pp')|\mathbf{ee}]$  defined in Eq. (3.8) for the reference atom at position  $\mathbf{e}$  and the projection of the Cartesian components onto the  $L=1$  angular momentum states

$$\begin{aligned} A_{\alpha M}^1 &= \delta_{\alpha x} \frac{1}{\sqrt{2}} (\delta_{M-1} - \delta_{M1}) \\ &+ \delta_{\alpha y} \frac{i}{\sqrt{2}} (\delta_{M1} + \delta_{M-1}) + \delta_{\alpha z} \delta_{M0}. \end{aligned} \quad (4.5)$$

The optical transition matrix elements from the  $A_G$  ground state to the electron-hole pair excited states introduced in Eq. (3.3) are

$$\langle LNP_e p_h | \hat{P}_\alpha | 0 \rangle = \delta_{L1} \delta_{p_e, -p_h} D(12|p_e p_h) A_{\alpha N}^1. \quad (4.6)$$

Selection rules limit excitations to  $L=1$  excitons with odd parity, i.e.,  $T_{1U}$  states<sup>10,12</sup>. Out of the 60 singlet excitons there are only six such states, namely,  $|1N+-\rangle$  and  $|1N-+\rangle$  with  $N=-1,0,1$ . Because of the different structures of the single-particle eigenvectors in Eq. (2.8), the oscillator strengths vary with the parity-allowed pairs

$$\begin{aligned} D(12|+-) &= -0.48547eR_0, \\ D(12|-+) &= -0.55626eR_0. \end{aligned} \quad (4.7)$$

The characteristic dipole length is about half the distance from a carbon atom to the center of the cage.

The coupling of two different excitonic states by an external electric field via the polarization operator is

$$\begin{aligned} \langle LNP_e p_h | \hat{P}_\alpha | L'N'p'_e p'_h \rangle &= \sum_{m_e, m'_e=-1}^{+1} \sum_{m_h, m'_h=-2}^{+2} (-1)^{-m_h-m'_h} C_{1m_e 2-m_h}^{LN} \\ &\times C_{1m'_e 2-m'_h}^{L'N'} \{ -\delta_{p_e p'_e} \delta_{m_e m'_e} \langle 2p'_h m'_h | ex_\alpha | 2p_h m_h \rangle \\ &+ \delta_{p_h p'_h} \delta_{m_h m'_h} \langle 1p_e m_e | ex_\alpha | 1p'_e m'_e \rangle \}. \end{aligned} \quad (4.8)$$

We record here a special case needed later for the nonlinear optical spectra, by Eq. (4.3),

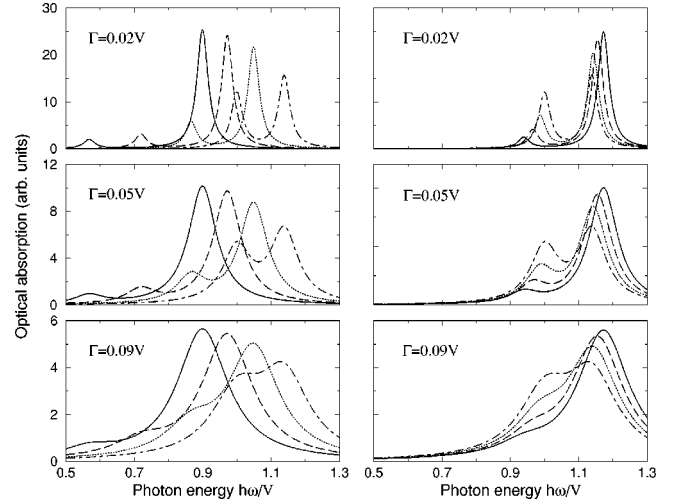


FIG. 6. Absorption spectra of  $C_{60}$  versus the photon energy in units of V for different parameters of the effective Coulomb interaction and damping parameters  $\Gamma$ . Solid line,  $U=3V$ ; dashed line,  $U=2V$ ; dotted line,  $U=1V$ ; dash-dotted line,  $U=0$ . The ratio of the intersite and intrasite Coulomb interaction is fixed to  $e^2/\epsilon R_0 U = 0.2377$  (left panel) and  $0.0517$  (right panel).

$$\begin{aligned} \langle 2Npp | \hat{P}_\alpha | 1N' - p' p' \rangle &= \sqrt{\frac{3}{20}} [\delta_{pp'} \sqrt{5} D(11|p-p) + \delta_{p,-p'} D(22|-pp)] \\ &\times (-1)^{N'} \sum_{M''=-1}^{+1} C_{2N1-N'}^{1M''} A_{\alpha M''}^1, \end{aligned} \quad (4.9)$$

with  $D(11|+-) = D(11|-+) = -0.70700eR_0$  and  $D(22|+-) = D(22|-+) = 0.75585eR_0$ . The dipole-allowed transitions from  $T_{1U}$  to both  $H_G$  and  $T_{1G}$  excitons are possible because of the difference of the  $C_{60}$  symmetry group from the spherical symmetry.

### B. Linear absorption: Optically allowed excitons

Consider the case of the  $A_G$  ground state. Its optical properties are governed by the time-dependent polarization field

$$P_\alpha(t) = 2n \langle 0 | \hat{P}_\alpha(t) | 0 \rangle, \quad (4.10)$$

where  $n$  is the density of the buckyballs. The linear response in the rotating-wave approximation is, following Eq. (4.6), given by

$$\chi_{\alpha\beta}^{(1)}(\omega) = \delta_{\alpha\beta} 2n \sum_{\Lambda=+,-} \frac{\left| \sum_{p=+,-} c_{\Lambda p} (1-) D(12|-pp) \right|^2}{E_{1-\Lambda} - \hbar\omega - i\Gamma_{1-\Lambda}}, \quad (4.11)$$

where  $\omega$  is the frequency of light and a phenomenological lifetime-broadening parameter  $\Gamma_{LP\Lambda}$  has been introduced for the electron-hole pair states. The diagonality and isotropy of the susceptibility tensor follows immediately from  $\sum_{M=-1}^{+1} A_{\alpha M}^1 A_{\beta M}^1 = \delta_{\alpha\beta}$ .

The resulting low-energy absorption spectrum of the  $\pi$ -electron system is shown in Fig. 6 for various values of the effective intra-atomic Coulomb interaction  $U$ . The ratio of the interatomic and intra-atomic Coulomb interaction has

been fixed at the values  $e^2/\epsilon R_0 U = 0.2377$  (left panel) and 0.0517 (right panel). Using an intrasite matrix element  $U = 17.3$  eV, the two values correspond to the cases of no screening of the interatomic interaction ( $\epsilon = 1$ ) and of intermediate screening ( $\epsilon = 4.6$ ). In the spectral range considered the absorption in the  $\pi$ -electron system exhibits two  $T_{1U}$  exciton peaks at about  $E_{1--} \approx V + 0.012U - 0.666(e^2/\epsilon R_0)$  and  $E_{1-+} \approx 1.139V + 0.039U - 0.488(e^2/\epsilon R_0)$  with different oscillator strengths.

A comparison of the calculated absorption spectrum with experiment leads to two salient points for discussion: (i) the comparison of the calculated and measured peak positions and (ii) the relative intensities of the two absorption peaks. The two calculated exciton peaks should be compared to the measured absorption peaks at 3.81 and 4.90 eV,<sup>40</sup> or 3.65 and 4.72 eV,<sup>41</sup> or 3.78 and 4.84 eV.<sup>42</sup> The weak structure observed at lower energies, in particular the weak peak at 2.73 eV, for solid  $C_{60}$  (Ref. 41) has been ascribed to dipole-forbidden transitions, which become partially allowed due to lattice fluctuations, interface effects, and/or internal electric fields. The same holds for the small structure occurring in the energy region of 2 eV in spectra of  $C_{60}$  isolated in a noble gas matrix.<sup>40</sup> The intense absorption band close to 5.96 eV (Ref. 41) or 5.87 eV (Ref. 42) possesses only a partial  $\pi$  character and is also beyond the scope of our study. The identification of the lower and upper  $T_{1U}$  excitons ( $L = 1, P = -$ ) with the two absorption peaks under consideration restricts the range for the values of the parameters  $U$  and  $e^2/\epsilon R_0$ . If we take the strong on-site interaction value  $U = 17.3$  eV, the dielectric constant varies drastically between  $\epsilon \approx 2$  (for the hopping parameter  $V = 4.62$  eV) and  $\epsilon \approx 10$  (for  $V = 3.83$  eV). With a weaker  $U \approx 10$  eV, the range of the dielectric constant is reduced to  $2.5 < \epsilon < 4.8$ .

The theoretical result that the absorption peak at lower energy possesses a smaller oscillator strength than the peak

at higher energy is in agreement with the experimental observation. Within the single-particle approximation, i.e., for  $U = 0$  and  $e^2/\epsilon R_0 = 0$ , the oscillator strengths of the two transitions  $h_u \rightarrow t_{1g}$  and  $h_g \rightarrow t_{1u}$  between molecule levels are similar, from Eq. (4.7). The reduction of the ratio of the oscillator strength of the lower-energy peak to that of the higher-energy peak may be understood in terms of the Coulomb coupling of the two  $T_{1U}$  excitons, as is evident from the presence of the eigenvectors  $c_{\Lambda p}(1-)$  from Eq. (3.16) in the oscillator strength of Eq. (4.11). Since the dipole matrix elements  $D(12|+-)$  and  $D(12|-+)$  have the same sign and nearly equal magnitudes, the oscillator strengths of the two  $T_{1U}$  excitations are governed by the relative sign of the coefficients  $c_{\Lambda p}(1-)$  and so by the sign of the coupling term  $V_{+-}(1-)$  in Eq. (3.10). The domination of the exchange term leads to  $V_{+-}(1-) < 0$  and hence the oscillator strength of the low-energy exciton at  $\hbar\omega = E_{1--}$  is reduced compared to the high-energy absorption at  $\hbar\omega = E_{1-+}$ . This shows not only that the relative strengths of the two exciton peaks are influenced by the Coulomb interaction but also that the intersite interaction is indispensable.

### C. Electro-optic Kerr effect: Electric-field-induced forbidden excitons

In the theoretical linear optical spectra, the parity selection rule excludes the same-parity transitions, such as those lowest in energy,  $h_u \rightarrow t_{1u}$ . They can, however, be induced by the application of a static electric field that mixes the even-parity excitons with the odd-parity excitons. The linear response to the external laser field of the electric polarization [Eq. (4.10)] to second order in an applied static electric field  $\mathbf{F}$  (the Kerr effect) is closely related to the third-order susceptibility, to be derived in Sec. IV D. By a similar derivation leading to Eq. (4.15), the static electric field effect on the linear optical response is given by

$$\chi_{\alpha\beta}^{(1)}(\omega) = 2nP_{\alpha\beta}(\hat{F}) \frac{F^2}{4} \sum_{L=1}^2 \sum_{\Lambda', \Lambda'' = \pm} \frac{S_{L\Lambda'}^* S_{L\Lambda''}}{(E_{1-\Lambda'} - E_{L+-})(E_{L+-} - \hbar\omega - i\Gamma_{L+-})(E_{1-\Lambda''} - E_{L+-})}, \quad (4.12)$$

with the prefactor depending on the direction of the applied static field denoted by its unit vector  $\hat{F}$  relative to the light polarization direction,

$$P_{\alpha\beta}(\hat{F}) = \frac{3}{10} (3\delta_{\alpha\beta} + \hat{F}_\alpha \hat{F}_\beta), \quad (4.13)$$

and the oscillator strength  $S_{L\Lambda}$  given in Eq. (4.17).

The selection rules  $\Delta L = 0, \pm 1$  confine the contributions to the Kerr effect from the  $H_G$  and  $T_{1G}$  excitons. Because of the random orientations of the  $C_{60}$  molecules in solutions or in the face-centered-cubic thin films,<sup>43-45</sup> the dependence of the field direction of the prefactor is in practice averaged out to  $P_{\alpha\beta}(\hat{F}) = \delta_{\alpha\beta}$ . Only in the case of the low-temperature simple cubic crystals of undoped  $C_{60}$  is there a chance of experimentally partially probing the polarization dependence. The four molecules per unit cell are rotated by an

angle  $\phi$  around a space diagonal axis  $[111]$ ,  $[1\bar{1}\bar{1}]$ ,  $[\bar{1}1\bar{1}]$ , or  $[\bar{1}\bar{1}1]$ . The angle of rotation is found to be  $\phi = 22^\circ - 26^\circ$ .<sup>43-45</sup>

The spectrum of the electro-optic Kerr effect is presented in Fig. 7 as a function of the reduced photon energy for different model parameters of the effective Coulomb interaction,  $U$  and  $e^2/\epsilon R_0$ . The electric field strength has been fixed at  $eFR_0/2V = 0.001$  to compare with the allowed transitions in zero field in Fig. 6, corresponding to  $2.6 \times 10^5$  V/cm for a hopping parameter of  $V = 4.626$  eV. The positions of the field-induced excitons are approximately given by  $E_{2+-} = 0.757V + 0.019U - 0.760e^2/\epsilon R_0$  for the  $H_G$  exciton or  $E_{1+-} = 0.757V + 0.0121U - 0.986e^2/\epsilon R_0$  for the  $T_{1G}$  exciton. Their energy difference is determined by the interatomic Coulomb interaction  $E_{2+-} - E_{1+-} \approx 0.226e^2/\epsilon R_0 \approx 0.93$  eV/ $\epsilon$ . For intermediate screening, it is smaller than the line

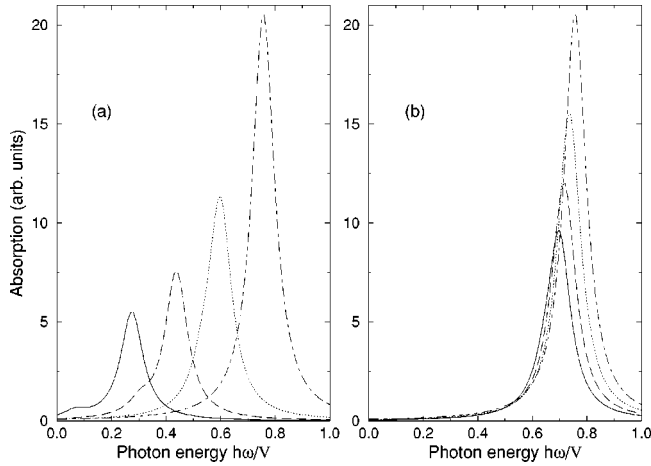


FIG. 7. Absorption spectra of  $C_{60}$  molecules in a static electric field versus the photon energy near the forbidden transition  $h_u \rightarrow t_{1u}$  for different parameters of the effective Coulomb interaction. Solid line,  $U=3V$ ; dashed line,  $U=2V$ ; dotted line,  $U=V$ ; dash-dotted line,  $U=0$ . (a)  $e^2/\epsilon R_0 U=0.2377$  and (b)  $e^2/\epsilon R_0 U=0.0517$ . The damping parameter is chosen as  $\Gamma=0.05V$ . Each spectrum has to be multiplied by the prefactor  $(eFR_0/2V)^2$  to compare with the strength in Fig. 6.

broadening used in Fig. 7, explaining the appearance of only one pronounced field-induced peak in the absorption spectrum below the energy of the lower allowed  $T_{1U}$  exciton (in Fig. 4). Only for very weak screening does a weak second  $T_{1G}$ -related peak appear at an energy below the more intense  $H_G$ -related peak [see the solid and dashed curves in Fig. 7(a)].

These general findings seem to be in agreement with the results inferred from different nonlinear optical experiments, such as two-photon absorption<sup>46</sup> and degenerate four wave mixing.<sup>47</sup> A two-photon resonance at 2.73 eV or 2.67 eV is observed and identified with an  $H_G$  exciton. Such energy values are within the range of the theoretical values given by the parameters under discussion. The prediction of a field-induced  $H_G$  exciton line also explains the weak absorption structure around 2.73 eV.<sup>41</sup> The theoretical energy ordering  $T_{1G} < H_G < T_{1U}$  clearly visible in Figs. 4 and 5 agrees with results of the second-harmonic generation on a surface,<sup>48,49</sup> where a resonance near 1.8–1.9 eV is identified with a  $T_{1G}$  exciton. However, the theoretical prediction of the energy splitting between  $T_{1G}$  and  $H_G$  is smaller than the experimental value of 0.8–0.9 eV if we choose our model parameters, such as  $U=17.3$  eV,  $\epsilon=4.6$ , to obtain similar exciton energies as the quantum-chemical calculations.

#### D. Third-harmonic generation

In this section we consider another nonlinear optical experiment, the third-harmonic generation (THG). A three-photon resonance occurs when three times the fundamental photon energy is equal to the lowest  $A_G \rightarrow T_{1U}$  one-photon dipole-allowed transition (in the single-particle picture  $h_u \rightarrow t_{1g}$  and  $h_g \rightarrow t_{1u}$ ). From the general expression for the third-order susceptibility given by Armstrong *et al.*,<sup>50</sup> we take into account only triply resonant contributions to the susceptibility describing THG. Neglecting biexciton effects<sup>51</sup> and using the dipole matrix elements (4.6) and (4.9) we find

$$\chi_{\alpha\beta\gamma\delta}^{(3)}(\omega) = \frac{2n}{3!} \mathcal{P}_{\beta\gamma\delta} \sum_{L=1}^2 \sum_{N=-L}^{+L} \sum_{N',N''=-1}^{+1} \sum_{\Lambda,\Lambda',\Lambda''=\pm 1} \langle 0 | \hat{P}_\alpha | 1N' - \Lambda' \rangle \times \frac{\langle 1N' - \Lambda' | \hat{P}_\beta | LN + \Lambda \rangle \langle LN + \Lambda | \hat{P}_\gamma | 1N'' - \Lambda'' \rangle \langle 1N'' - \Lambda'' | \hat{P}_\delta | 0 \rangle}{(E_{1-\Lambda'} - 3\hbar\omega - i\Gamma_{1-\Lambda'}) (E_{L+\Lambda} - 2\hbar\omega - i\Gamma_{L+\Lambda}) (E_{1-\Lambda''} - \hbar\omega - i\Gamma_{1-\Lambda''})}. \quad (4.14)$$

Here  $n$  is the density [cf. Eq. (4.10)] and  $\mathcal{P}_{\beta\gamma\delta}$  denotes the sum over all permutations of  $\beta$ ,  $\gamma$ , and  $\delta$  ensuring that the fourth-rank tensor third-order susceptibility is independent of the ordering of those three indices, i.e., the Cartesian components of the three fields creating the third-order harmonic.

Selection rules dictate that the three-photon resonance takes the system from the  $A_G$  ground state to the  $L=1$  excitons with odd parity ( $T_{1U}$ ) and from  $T_{1U}$  to  $L=2$  ( $H_G$ ) and  $L=1$  ( $T_{1G}$ ) excitons with even parity, which may give rise to the doubly resonant terms. We restrict ourselves to the double-resonance terms with the lower-energy ( $\Lambda = -$ ) excitons. The higher-lying excitons are energetically well separated from the frequency region of interest (cf. Fig. 4). Consequently, the  $|LN+-\rangle$  states may be approximately replaced by the uncoupled  $|LNPp\rangle$  ( $p = +, L=1,2$ ) states, corresponding to the single-particle transitions  $h_u \rightarrow t_{1u}$ . The third-order susceptibility becomes

$$\chi_{\alpha\beta\gamma\delta}^{(3)}(\omega) = 2n G_{\alpha\beta\gamma\delta} \sum_{L=1}^2 \sum_{\Lambda',\Lambda''=\pm} \frac{S_{L\Lambda'}^* S_{L\Lambda''}}{(E_{1-\Lambda'} - 3\hbar\omega - i\Gamma_{1-\Lambda'}) (E_{L+-} - 2\hbar\omega - i\Gamma_{L+-}) (E_{1-\Lambda''} - \hbar\omega - i\Gamma_{1-\Lambda''})}, \quad (4.15)$$

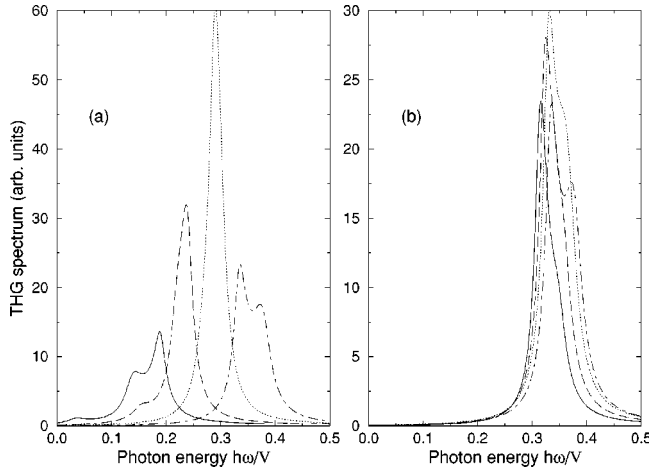


FIG. 8. Spectral variation of the THG susceptibility in the region of the lower three-photon  $T_{1U}$  and two-photon  $H_G$  resonances for the same parameters of the effective Coulomb interaction as in Fig. 7. The damping parameter is chosen as  $\Gamma=0.03V$  for both allowed and forbidden excitons.

with the polarization-dependent prefactor

$$G_{\alpha\beta\gamma\delta} = \frac{1}{8} P_{\beta\gamma\delta} \sum_{M=-2}^{+2} F_{\alpha\beta}^*(M) F_{\delta\gamma}(M),$$

$$F_{\alpha\beta}(M) = \sum_{M', M''=-1}^{+1} (-1)^{M'} A_{\alpha M'}^1 C_{2M1-M'}^{1M''} A_{\beta M''}^1 \quad (4.16)$$

and the oscillator strength

$$S_{L\Lambda} = \left[ \frac{1}{\sqrt{5-2L}} c_{\Lambda+} (1-) D(11|+-) + \sqrt{\frac{5-2L}{5}} c_{\Lambda-} (1-) D(22|-+) \right] \times \sum_{p=\pm} c_{\Lambda p}^* (1-) D(12|-pp). \quad (4.17)$$

Equation (4.15) may be interpreted as the third-order susceptibility of a five-level system: ground state  $A_G$ , even-parity excited states  $H_G$  or  $T_{1G}$ , and the two odd-parity excited states  $T_{1U}$ , in contrast to the third-order susceptibility of a three-level system used to fit the experimental measurements.<sup>52,53</sup> Moreover, the symmetry of the states participating in the THG process are well defined here. On the other hand, only the most dominant resonant terms are considered here, whereas the formulas used to fit the data also include less important resonant and nonresonant terms.

The spectral behavior of the magnitude of the third-order susceptibility is plotted in Fig. 8 for the same set of model parameters as in Fig. 7. Only the lower  $T_{1U}$  excitons appear. Despite the presence of many exciton levels, in the spectral region considered only a pronounced double-peak structure or one broad peak appears. In the case of stronger screening of the intersite Coulomb interaction (the right panel of Fig. 8), the high-energy peak corresponds to the two-photon resonance with the  $L=2, P=+$  ( $H_G$ ) exciton. It is enhanced by

the resonance with the  $T_{1G}$  excitons ( $L=1, P=+$ ). The three-photon resonance at the frequency of the fundamental light wave occurs at slightly lower energies defined by the electric-dipole-allowed  $L=1, P=-$  ( $T_{1U}$ ) exciton. On the other hand, in the case of the weaker screening (the left panel), for the curves going from the right to the left in order of increasing on-site Coulomb interaction  $U$ , there is an interchange of the energy order of the two resonances  $\hbar\omega = \frac{1}{3}E_{1--}$  and  $\hbar\omega = \frac{1}{2}E_{2+-}, \frac{1}{2}E_{1+-}$ . The near coincidence of the triple and double resonances for the intermediate values of  $U$  creates the appearance of a strong single peak in Fig. 8(a). For larger values of the on-site Coulomb interaction, the  $H_G$  and  $T_{1G}$  resonances split again and a weak  $T_{1G}$ -related peak occurs at the low-energy tail of the THG structure.

Our calculated spectrum can be used to infer the symmetry of two-particle elementary excitations observed experimentally. In the THG experiment<sup>52,53</sup> two peaks were observed at 1.3  $\mu\text{m}$  and 1.06  $\mu\text{m}$ . By taking a combination of relatively large parameters  $V$ ,  $U$ , and  $e^2/\epsilon R_0$ , we can interpret the lower two-photon resonance to yield the measured energy of the  $H_G$  exciton at 1.9 eV and the higher triple-photon resonance to yield the energy of the  $T_{1U}$  exciton at 3.5 eV. A previous interpretation of the low-energy peak in the THG spectrum as a two-photon resonance with the one-photon forbidden  $T_{1G}$  level,<sup>52</sup> even though in agreement with the low value of the resonance energy, could not explain the absence of the  $H_G$  exciton in the spectrum. We have demonstrated here that, with the help of a careful symmetry analysis, nonlinear optical spectroscopy can clarify the complicated electronic structure of the  $C_{60}$  molecule, especially its electron-hole pair excitations.

## V. DISCUSSION

In this paper we address the issue of the strong electron correlation in a  $C_{60}$  molecule by studying the effects of the excitons using an analytical model making maximum use of symmetry. The basic component is a simple quasiparticle model based on a tight-binding scheme of  $\pi$  orbitals of the HOMO and LUMO states, with parameters deduced from photoemission and inverse photoemission experiments. The assumption of the closed-shell ground state is tested against the energies of the electron-hole pair excited states. The interaction between electrons and holes includes the Coulomb interaction of the  $\pi$  orbitals on the same carbon atom and the long-range interaction between different carbon sites with a constant dielectric screening. The on-site electron-hole interaction is dominated by the exchange term and is therefore repulsive while the electron-hole interaction on different carbon sites is attractive. The screening of the latter is more important in determining the energy levels of the excitons.

Our theory of the linear optical absorption spectra based on the closed-shell ground state agrees with experiment for a reasonably strong dielectric screening of the long-range interaction. We have established the relation between the energies or relative oscillator strengths of the dipole-active excitons and the Coulomb interaction terms connecting these excitons of the same symmetry. This coupling effect explains the observed strong  $T_{1U}$  exciton peaks in the linear optical absorption spectra. For the third-harmonic generation, our

theory identifies the doublet excitation at the fundamental wavelength  $\lambda \approx 1.3 \mu\text{m}$  as the forbidden  $H_G$  exciton and not as the  $T_{1G}$  exciton suggested by experiment, whereas the triple resonance is clearly related to the  $T_{1U}$  excitation. This identification is supported by the argument invoking the approximate angular momentum selection rule in the nearly centrosymmetric molecule (see Sec. IV). The same transition to the  $H_G$  pairs is found to play a role if an external static electric field is applied to the  $C_{60}$  molecules. We predict a pronounced optical Kerr effect with a photon resonance at the  $H_G$  energy.

Our model approach may also be used to study excitons and their effects on optical properties in other molecular solids, clusters, and quantum dots, the last particularly when the effective-mass approximation fails. While our study indicates that the closed-shell  $A_G$  is the ground state in  $C_{60}$ , it is of interest to investigate whether an excitonic state of lower symmetry than the closed-shell state might be the lowest energy state in other systems. Such an event is known as symmetry breaking. To use the  $C_{60}$  as a temporary paradigm, we note that the closed-shell  $A_G$  state would be unstable against an electron-hole pair excitation of symmetry  $T_{2G}$  if either the gap between LUMO and HOMO or the interatomic interaction were reduced. The consequences of having a lower symmetry exciton state, such as  $T_{2G}$ , as the ground state are extraordinary. The optically dipole-allowed states would no longer be of  $T_{1U}$  symmetry but  $H_U$  or  $G_U$ . The

most interesting possibility is that a quasiparticle state now consists of an electron (or hole) plus an electron-hole pair, leading to strong correlation effects. Symmetry consideration would lead to more photoemission lines than the closed-shell ground state scenario. The interpretation of the THG would be different. A three-photon resonance would excite the  $H_U$  or  $G_U$  exciton. Many transitions could contribute to the two-photon resonance, such as  $H_U \rightarrow T_{1G}$ ,  $H_G$ ,  $T_{2G}$ , and  $G_G$  or  $G_U \rightarrow H_G$ ,  $T_{2G}$ , and  $G_G$ . An experimental test of the electro-optic effect (Sec. IV C) could discriminate the ground state symmetry.

Even in a less extreme case of a small but positive excitation energy of the  $T_{2G}$  exciton, the quasiparticle dynamics can be affected by the easy Coulomb excitation of such excitons. In particular, this could provide a source of effective quasiparticle interaction and thus possibly a source for superconductivity. We leave the investigation of the above conjectures to future work.

#### ACKNOWLEDGMENTS

One of the authors (F.B.) gratefully acknowledges the kind hospitality of the University of California at San Diego. This work was financially supported by the Volkswagen Foundation and the National Science Foundation (NSF) (Grant Nos. INT-9513363, DMR-9421966, and DMR-9721444).

- <sup>1</sup>H. W. Kroto, J. R. Heath, S. C. O'Brien, R. F. Curl, and R. E. Smalley, *Nature (London) (London)* **318**, 162 (1985).
- <sup>2</sup>A. F. Hebbard, M. J. Rosseinsky, R. C. Haddon, D. W. Murphy, S. H. Glarum, T. T. M. Palstra, A. P. Ramirez, and A. R. Kortan, *Nature (London)* **350**, 600 (1991); K. Holczer, O. Klein, S.-M. Huang, R. B. Kaner, K.-J. Fu, R. L. Whetten, and F. Diederich, *Science* **252**, 1154 (1991); M. J. Rosseinsky, A. P. Ramirez, S. H. Glarum, D. W. Murphy, R. C. Haddon, A. F. Hebard, T. T. M. Palstra, A. R. Kortan, S. M. Zahurak, and A. V. Makhija, *Phys. Rev. Lett.* **66**, 2830 (1991); K. Tanigaki, T. W. Ebbesen, S. Saito, J. Mizuki, J. S. Tsai, Y. Kubo, and S. Kuroshima, *Nature (London)* **352**, 222 (1991).
- <sup>3</sup>P.-M. Allemand, K. C. Khemani, A. Koch, F. Wudl, K. Holczer, S. Donovan, G. Grüner, and J. D. Thompson, *Science* **253**, 301 (1991).
- <sup>4</sup>R. W. Lof, M. A. van Veenendaal, B. Koopmans, H. T. Jonkman, and G. A. Sawatzky, *Phys. Rev. Lett.* **68**, 3924 (1992).
- <sup>5</sup>B. Friedman and J. Kim, *Phys. Rev. B* **46**, 8638 (1992).
- <sup>6</sup>J. M. Dong, Z. D. Wang, D. Y. Xing, Z. Domanski, Zbigniew Domanski, Paul Erdős, and P. Santini, *Phys. Rev. B* **54**, 13 611 (1996), and references therein.
- <sup>7</sup>P. E. Lammert, D. S. Rokhsar, S. Chakravarty, S. Kivelson, and M. I. Salkola, *Phys. Rev. Lett.* **74**, 996 (1995), and references therein.
- <sup>8</sup>R. Friedberg, T. D. Lee, and H. C. Ren, *Phys. Rev. B* **46**, 14 150 (1992).
- <sup>9</sup>S. Leach, M. Vervloet, A. Després, E. Breheret, J. P. Hare, T. J. Dennis, H. W. Kroto, R. Taylor, and D. R. M. Walton, *Chem. Phys.* **160**, 451 (1992).
- <sup>10</sup>I. László and L. Udvardi, *Chem. Phys. Lett.* **136**, 418 (1987); J. Mol. Struct.: THEOCHEM **183**, 271 (1989).
- <sup>11</sup>R. D. Bendale, J. D. Baker, and M. C. Zerner, *Int. J. Quantum Chem., Symp.* **25**, 557 (1991).
- <sup>12</sup>F. Negri, G. Orlandi, and F. Zerbetto, *J. Chem. Phys.* **97**, 6496 (1992).
- <sup>13</sup>F. Bechstedt, *Adv. Phys.* **32**, 161 (1992).
- <sup>14</sup>E. L. Shirley and S. G. Louie, *Phys. Rev. Lett.* **71**, 133 (1993); S. G. Louie and E. L. Shirley, *J. Phys. Chem. Solids* **54**, 1767 (1993).
- <sup>15</sup>S. Saito and A. Oshiyama, *Phys. Rev. Lett.* **66**, 2637 (1991).
- <sup>16</sup>W. Y. Ching, Ming-Zhu Huang, Yong-Nian Xu, W. G. Harter, and F. T. Chan, *Phys. Rev. Lett.* **67**, 2045 (1991).
- <sup>17</sup>C. M. Varma, J. Zaanen, and K. Raghavachari, *Science* **254**, 989 (1991).
- <sup>18</sup>M. Schlüter, M. Lannoo, M. Needels, G. A. Baraff, and D. Tomanek, *Phys. Rev. Lett.* **68**, 526 (1992).
- <sup>19</sup>E. L. Shirley, L. X. Benedict, and S. G. Louie, *Phys. Rev. B* **54**, 10 970 (1996).
- <sup>20</sup>R. F. Curl and R. E. Smalley, *Sci. Am. (Int. Ed.)* **265** (4), 32 (1991).
- <sup>21</sup>R. C. Haddon, L. E. Brus, and K. Raghavachari, *Chem. Phys. Lett.* **125**, 459 (1986).
- <sup>22</sup>D. A. Bochvar and E. G. Gal'pern, *Dokl. Akad. Nauk SSSR* **209**, 610 (1973).
- <sup>23</sup>Y. Deng and C. N. Yang, *Phys. Lett. A* **170**, 116 (1992).
- <sup>24</sup>L. J. Sham and T. M. Rice, *Phys. Rev.* **144**, 708 (1966).
- <sup>25</sup>N. Laouini, O. K. Andersen, and O. Gunnarsson, *Phys. Rev. B* **51**, 17 446 (1995).
- <sup>26</sup>M. Hamermesh, *Group Theory and Its Application to Physical Problems* (Addison-Wesley, Reading, MA, 1962).

- <sup>27</sup>D. A. Varshalovich, A. N. Moskalev, and V. K. Khersonskii, *Quantum Theory of Angular Momentum* (World Scientific, Singapore, 1988).
- <sup>28</sup>T. Takahashi, S. Suzuki, T. Morikawa, H. Katayama-Yoshida, S. Hasegawa, H. Inokuchi, K. Seki, K. Kikuchi, S. Suzuki, K. Ike-moto, and Y. Achiba, *Phys. Rev. Lett.* **68**, 1232 (1992).
- <sup>29</sup>J. H. Weaver, J. L. Martins, T. Komeda, Y. Chen, T. R. Ohno, G. H. Kroll, N. Troullier, R. E. Haufler, and R. E. Smalley, *Phys. Rev. Lett.* **66**, 1741 (1991); J. H. Weaver, P. J. Benning, F. Stepniak, and D.M. Poirier, *J. Phys. Chem. Solids* **53**, 1707 (1992).
- <sup>30</sup>P. J. Benning, J. L. Martins, J. H. Weaver, L. P. F. Chibante, and R. E. Smalley, *Science* **252**, 1417 (1991).
- <sup>31</sup>In the standard spectroscopic notation an additional upper index  $2S+1$ , which gives the multiplicity of the states, is necessary for a complete characterization. However, in the considered case of singlet states ( $S=0$ ) the multiplicity is fixed to the value 1 and hence may be omitted.
- <sup>32</sup>R. G. Parr, *Quantum Theory of Molecular Electronic Structure* (Benjamin, New York, 1963), pp. 51. and 247.
- <sup>33</sup>S. Ishibashi, N. Terada, M. Takumoto, N. Kinoshita, and H. Ihara, *J. Phys. Chem.* **4**, L169 (1992).
- <sup>34</sup>P. Ecklung, *Bull. Am. Phys. Soc.* **37**, 191 (1992); A. F. Hebard, R. C. Haddon, R. M. Fleming, and A. R. Kortan, *Appl. Phys. Lett.* **59A**, 2109 (1991).
- <sup>35</sup>Y.-N. Xu, M.-Z. Huang, and W. Y. Ching, *Phys. Rev. B* **44**, 13 171 (1991).
- <sup>36</sup>Ph. Lambin, A. A. Lucas, and J.-P. Vigneron, *Phys. Rev. B* **46**, 1794 (1992).
- <sup>37</sup>G. Cappellini, F. Bechstedt, A. Bosin, and F. Casula, *Phys. Status Solidi B* **189**, 1534 (1995).
- <sup>38</sup>P. L. Hansen, P. J. Fallon, and W. Krättschmer, *Chem. Phys. Lett.* **181**, 367 (1991).
- <sup>39</sup>C. Hartmann, M. Zigone, G. Martinez, E. L. Shirley, L. X. Benedict, S. G. Louie, M. S. Fuhrer, and A. Zettl, *Phys. Rev. B* **52**, R5550 (1995).
- <sup>40</sup>Z. Gasyna, P. N. Schatz, J. P. Hare, T. J. Dennis, H. W. Kroto, R. Taylor, and D. R. M. Walton, *Chem. Phys. Lett.* **183**, 283 (1991).
- <sup>41</sup>S. L. Ren, Y. Wang, A. M. Rao, E. McRae, J. M. Holden, T. Hager, KaiAn Wang, W.-T. Lee, H. F. Ni, J. Selegue, and P. C. Eklund, *Appl. Phys. Lett.* **59**, 2678 (1991).
- <sup>42</sup>H. Ajje, M. M. Alvarez, S. J. Anz, R. D. Beck, F. Diederich, F. Fostiropoulos, D. R. Huffman, W. Krättschmer, Y. Rubin, K. E. Schriver, D. Sensharma, and R. L. Whetten, *J. Phys. Chem.* **94**, 8630 (1990).
- <sup>43</sup>P. A. Heiney, J. E. Fischer, A. R. Mcghie, W. J. Romanow, A. M. Denenstein, J. P. McCauley, Jr., A. B. Smith, and D. E. Cox, *Phys. Rev. Lett.* **66**, 2911 (1991).
- <sup>44</sup>R. Sachidanandam and A. B. Harris, *Phys. Rev. Lett.* **67**, 1467 (1991).
- <sup>45</sup>W. I. F. David, R. M. Ibberson, J. C. Matthewman, K. Prassides, T. John, S. Dennis, J. P. Hare, H. W. Kroto, R. Taylor, and D. M. R. Walton, *Nature (London) (London)* **353**, 147 (1991).
- <sup>46</sup>G. P. Banfi, D. Fortusini, M. Bellini, and P. Milani, *Phys. Rev. B* **56**, R10 075 (1997).
- <sup>47</sup>F. P. Strohkendl, R. L. Larsen, T. Axenson, R. L. Dalton, R. W. Hellwarth, H. Sarkas, and Z. H. Kafafi, *Proc. SPIE* **2854**, 191 (1996).
- <sup>48</sup>B. Koopmans, A.-M. Janner, H. T. Jonkman, G. A. Sawatzky, and F. van der Woude, *Phys. Rev. Lett.* **71**, 3569 (1993).
- <sup>49</sup>A.-M. Janner, R. Eder, B. Koopmans, H. T. Jonkman, and G. A. Sawatzky, *Phys. Rev. B* **52**, 17 158 (1995).
- <sup>50</sup>J. A. Armstrong, N. Bloembergen, J. Ducuing, and P. Pershan, *Phys. Rev.* **127**, 1918 (1962).
- <sup>51</sup>See, for example, Th. Östreich, K. Schönhammer, and L. J. Sham, *Phys. Rev. Lett.* **74**, 4698 (1995).
- <sup>52</sup>F. Kajzar, C. Taliani, R. Danielli, S. Rossini, and R. Zamboni, *Chem. Phys. Lett.* **217**, 418 (1994).
- <sup>53</sup>F. Kajzar, C. Taliani, R. Zamboni, S. Rossini, and R. Danielli, *Proc. SPIE* **2025**, 352 (1993).